Page Proof Instructions and Queries

Thank you for choosing to publish with us. This is your final opportunity to ensure your article will be accurate at publication. Please review your proof carefully and respond to the queries using the circled tools in the image below, which are available in Adobe Reader DC* by clicking **Tools** from the top menu, then clicking **Comment.**

Please use *only* the tools circled in the image, as edits via other tools/methods can be lost during file conversion. For comments, questions, or formatting requests, please use $\boxed{T}$ Please do *not* use comment bubbles/sticky notes 💬.

Comment ▾ 💬 ✏️ T T T T T T ✏️ 🧽 📑 📎 🔖
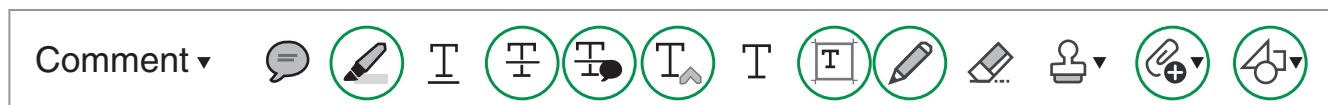
*If you do not see these tools, please ensure you have opened this file with Adobe Reader DC, available for free at get.adobe.com/reader or by going to Help > Check for Updates within other versions of Reader. For more detailed instructions, please see us.sagepub.com/ReaderXProofs.

No.	Query
	Please note, only ORCID iDs validated prior to acceptance will be authorized for publication; we are unable to add or amend ORCID iDs at this stage.
	Please confirm that all author information, including names, affiliations, sequence, and contact details, is correct.
	Please review the entire document for typographical errors, mathematical errors, and any other necessary corrections; check headings, tables, and figures.
	Please confirm that the Funding and Conflict of Interest statements are accurate.
	Please ensure that you have obtained and enclosed all necessary permissions for the reproduction of artistic works, (e.g. illustrations, photographs, charts, maps, other visual material, etc.) not owned by yourself. Please refer to your publishing agreement for further information.
	Please note that this proof represents your final opportunity to review your article prior to publication, so please do send all of your changes now.

The effect of loading rate on the compression properties of carbon fibre-reinforced epoxy honeycomb structures

RA Alia[1] , J Zhou[2] , ZW Guan[3,4], Q Qin[5], Y Duan[2] and WJ Cantwell[1]

Abstract

The effect of varying strain rate on the compression strength and energy absorption characteristics of a carbon fibre-reinforced plastic honeycomb core has been investigated over a wide range of loading rates. The honeycombs were manufactured by infusing an epoxy resin through a carbon fibre fabric positioned in a dismountable honeycomb mould. The vacuum-assisted resin transfer moulding technique yielded honeycomb cores of a high quality with few defects. Compression tests were undertaken on single and multiple cells and representative volumes removed from the cores in order to assess how the compression strength and specific energy absorption vary with test rate. Crushing tests over the range of strain rates considered highlighted the impressive strength and energy-absorbing response of the honeycomb cores. At quasi-static rates of loading, the compression strength and specific energy absorption characteristics of the unidirectional samples exceeded those of the multidirectional cores. Here, extensive longitudinal splitting and fibre fracture were the predominant failure mechanisms in the cores. For all three stacking sequences, the single-cell samples offer higher compression strength than their five-cell counterparts. In contrast, the specific energy absorption values were found to be slightly higher in the five-cell cores. The experiments highlighted a trend of increased compression strength with loading rate in the multidirectional samples, whereas the strength of the $[0°]_4$ samples was relatively insensitive to strain rate. Finally, the energy absorbing capacity of all structures studied was found to be reasonably constant at increasing rates of strain.

Introduction

Lightweight sandwich structures, based on composite skins bonded to a low-density core, are currently being used in a range of lightweight aircraft structures. Traditionally, the core material in such structures takes the form of a honeycomb design, such as Nomex (aramid fibre/phenolic resin) and aluminium foil-based systems.

A number of investigations[1–10] have been conducted to study the crushing behaviour of honeycomb structures under compressive loads over a wide range of strain rates. Wu and Jiang[2] investigated the static and dynamic characteristics of aluminium honeycomb in the axial direction. They showed that the crush strength increases by up to 74% under dynamic loading relative to static loading, with more irregular folding mechanisms being observed in the impacted samples.

Similar experimental observations were noted in the work carried out by Zhao and Gary,[5] where out-of-plane dynamic crushing resulted in an increase up to 40% in compression strength relative to quasi-static loading conditions. Wang et al.[7] studied the high-velocity impact response of hexagonal aluminium honeycomb cores over a range of velocities ranging from 20 m/s to 80 m/s. The experiments revealed that the plateau stress increases significantly at impact velocities below 30 m/s. As the velocity was increased from 30 to 80 m/s, steady slow increments in the plateau stress were observed. The crushing behaviour of aluminium and Nomex honeycomb structures under transverse loading was investigated both experimentally and numerically by Aktay et al.[9] They showed that in contrast to the progressive folding failure mode observed in aluminium honeycomb, the failure initiation and propagation characteristics of Nomex involve buckling of cell walls, debonding of the cell interfaces and fracture of the phenolic resin layer.

Significant efforts have been made to study the mechanical behaviour of composite core structures, involving various composite cell topologies, including pyramidal, Kagome lattice, tetrahedral and egg-box.[11–17] Finnegan et al.[11] manufactured and tested carbon fibre-reinforced plastic (CFRP) pyramidal truss structures with pre-fabricated composite face sheets. Compression test data showed that the structures failed mainly by truss push-out through the composite face sheets, suggesting that the use of thicker face sheets may overcome this issue. CFRP Kagome lattice structures based on interlocking method were fabricated by Fan et al.[12,13] A number of researchers[14,15] subsequently designed and evaluated the energy absorbing capability of hierarchical square lattice composites. A plastic model was developed to predict the limits of the deformation plateau. Xiong et al.[16,17] investigated the quasi-static crushing response of carbon fibre composite egg and pyramidal core structures fabricated using an interlocking method. They found that the 3D grid core sandwich panels absorbed energy primarily through a progressive crushing mode.

In recent years, a significant number of studies have been conducted that focus on manufacturing composite honeycombs and studying their mechanical performance.[18–23] The mechanical behaviour of flax fibre-reinforced polymeric honeycomb cores manufactured using matched-die compression moulding was investigated by Petrone et al.[18,19] They reported that the mechanical response of continuous fibre-reinforced composites cores are superior to that of short fibre-reinforced samples when subjected to impact loading. The crushing response of square composite honeycomb cores has been investigated by Russell et al.[20,21] and Park et al.[22] More recently, Vitale et al.[23] attempted to fabricate natural and synthetic fibre-reinforced honeycomb sandwich panels using the vacuum-assisted resin transfer moulding (VARTM) technique. In order to construct a predictive failure map for the sandwich structures, various failure mechanisms were considered, including face wrinkling, face yielding, core shear and core crushing. Alia et al.[24] manufactured carbon fibre-reinforced epoxy honeycomb cores using a steel mould and the VARTM technique. The influence of stacking configurations, weight fraction of fibres and the effect of chamfering on specific energy absorption (SEA) and compressive strength was investigated. The aim of the current paper is to investigate strain rate effects in the compressive behaviour of honeycomb cores based on a carbon fibre-reinforced epoxy resin. The cores are manufactured by using the VARTM method to infuse a honeycomb mould. Attention is given to assessing the effect of strain rate on the compressive and energy-absorbing characteristics of the composite cores and elucidating the failure mechanisms over the range of strain rates considered.

Experimental procedure

Sample preparation

The composite honeycomb cores studied here were prepared from a 12 k unidirectional carbon fibre cloth (Unitex UT-300/500) and a room-temperature curing epoxy resin system. The carbon fibre fabric used as the reinforcement had an areal density of approximately 290 g/m^2, a nominal thickness of 0.25 mm and was supplied in the form of a continuous wide roll with a width of 500 mm. The epoxy resin was a two-part, toughened epoxy system, Prime^{TM} 20LV with a glass transition temperature of 68°C. Both the carbon fibre fabric and the epoxy resin were supplied by Gurit Ltd.

Honeycomb cores were prepared using a steel mould consisting of a baseplate and insertable hexagonal blocks, as shown in Figure 1. Here, a total of 39 hexagon-shaped steel blocks with a height of 27 mm, with a face-to-face dimension of 27 mm, were inserted into machined grooves in the mould baseplate, Figure 1(a). The slots in the baseplate were machined to yield spacings equal to either 1.5 mm or 3.0 mm, depending on the location within the mould, Figure 1(b). After positioning the hexagonally-shaped blocks on the baseplate, four strips of carbon fibre fabric, with a height of 22 mm, were inserted into the openings in the mould, as can be seen in Figure 1(c). Inserting four layers of carbon fibre fabric resulted in the composite exhibiting a nominal fibre weight fraction of 0.49. The hexagonal mould was placed on a large glass table and wrapped in a vacuum bag in preparation for resin infusion, Figure 1(d).
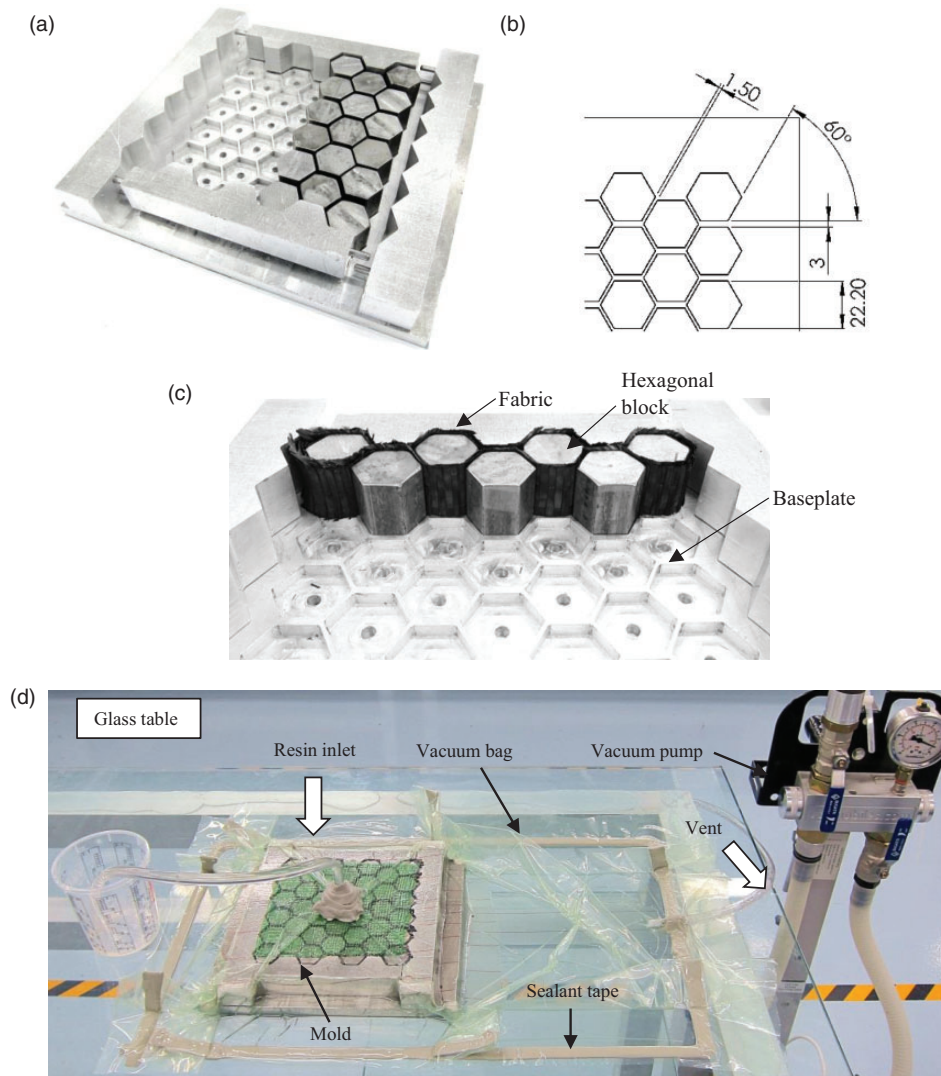
Figure 1. (a) Mould, (b) base plate spacings, (c) carbon fibre fabric with a height of 22 mm were inserted into the openings in the mould and (d) infusion setup.

The resin infusion process was undertaken at room temperature and facilitated by a line injection and a line vent. The process required approximately 30 min to complete. The epoxy resin in the honeycombs was then allowed to cure under vacuum for a period of 24 h. After curing, the bagging material was removed, and the steel blocks were pushed out of the honeycomb yielding a high-quality core structure, such as that shown in Figure 2(a). In the initial part of this study, attention focused on a unidirectional honeycomb with the fibres in the four unidirectional plies being parallel to each other in the 0° (through-the-thickness) direction. Clearly, such composites exhibit reduced properties in the transverse direction and are prone to splitting when loaded in compression. In order to avoid this undesirable failure mode, honeycombs were also produced with the central layers oriented at either ±45° or

90° yielding cores, with stacking sequences of [0°, −45°, +45°, 0°] or [0°, [90°]$_2$, 0°], respectively.

Quasi-static compression testing

In preparation for mechanical testing, the honeycomb core structures were cut using a conventional band-saw to yield specimens based on one and five hexagonal cells, Figure 2(b) and (c). The compression strength and energy-absorbing response of the test samples were evaluated at crosshead displacement rates of 0.2, 2, 20 and 100 mm/min using an MTS universal testing machine with a load capacity of 250 kN. The force and displacement graphs' data were recorded during each test. The resulting data, coupled with the initial mass of the sample, were then used to calculate the SEA capability of the hex-core samples. The absorbed energy
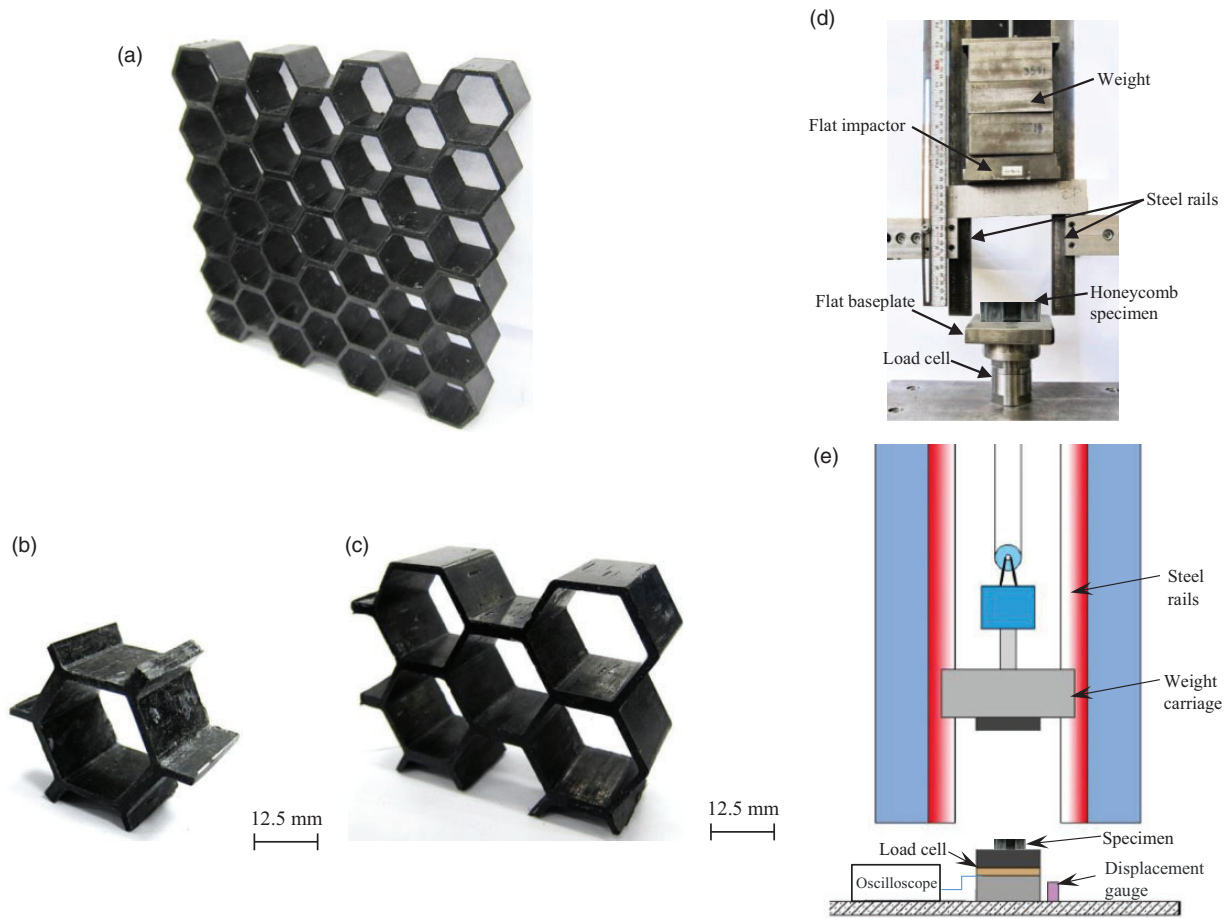
Figure 2. (a) Photograph of a manufactured sample, photograph of (b) one- and (c) five-cell honeycomb core samples, (d) the small drop-weight impact test setup and (e) the schematic of 30 meter drop-weight impact test setup.

was determined from the energy under the load–displacement trace up to the point where the curve begins to rise rapidly and normalized by the specimen mass.

Dynamic testing

The dynamic mechanical characteristics of samples consisting of either one or five hexagonal cells were evaluated by conducting drop-weight crushing tests. Prior to testing, the one-cell hexagonal specimens were placed on a flat steel baseplate of an impact tower (located at the University of Liverpool), directly above a 100 kN Kistler type 9363A load cell, as shown in Figure 2(d). Initially, the impactor, with a flat loading plate with dimensions of 120 mm × 80 mm, was raised to a predefined height, depending on the velocity and impact energy required. The drop mass was guided by two steel rails, and the maximum drop height adopted was 1.2 m. A high-speed video camera (MotionPro X4, type X4CU-U-4 with an F/0.95–50 mm lens) was employed to record the displacement

and elucidate the failure mechanisms in the honeycomb structure. Due to the limited capacity of the load cell and energy capability of the universal drop-weight tower, the five-cell honeycomb samples were tested using a heavy duty DHR-1205 drop-hammer impact tower (located at Xian Jiaotong University), as shown in Figure 2(e). The DHR-1205 offers the following capability, a maximum height of 30 m, a hammer mass that can be varied from 15 to 1000 kg, a maximum impact velocity of 23.5 m/s and a maximum impact energy of 260,000 J. The specimens were positioned on a circular steel plate located above a 250 kN load cell and crushed by a circular steel plate fixed to a drop carriage. The mass of the carriage was varied from 39.6 to 87.67 kg and the impact energy from 350 J to 1200 J in order to fully crush the test samples. The load–displacement graphs were captured to evaluate the dynamic compression properties and energy absorption characteristics of the honeycomb core structures. The displacement was recorded using a Micro-Epsilon OptoNCDT 2300 high speed, high accuracy laser sensor with a 40 kHz sampling capability. The impact force was captured using

a piezoelectric load-cell and a Tektronix DPO2014B oscilloscope with a bandwidth of 100 MHz and a sample rate of 1GS/s, respectively. The force–displacement data were combined and analysed using the Matlab and Origin software packages. A high-speed video camera was used to record the crushing process of the honeycomb structures during testing. After testing, the residual height of the samples was measured to quantify the degree of crush.

Results and discussion

Quasi-static tests on the CFRP honeycombs

In the initial part of this investigation, the strength and energy-absorbing characteristics of single-cell honeycomb samples, based on four ply cores, were investigated through a series of quasi-static tests at a crosshead displacement rate of 0.2 mm/min, and the results of these tests are given in Table 1. Figure 3 shows typical load–displacement graphs of single-cell honeycomb following tests on samples with fibre stacking sequences of $[0°]_4$, $[0°, -45°, +45°, 0°]$ and $[0°, 90°]s$. Initially, the curves exhibit a rapid increase in load up to the peak value, with the unidirectional honeycomb offering the highest peak force of approximately 62 kN. Following the maximum in the trace, the

force decreases as the honeycombs were continuously compressed until reaching a point where the curve begins to rise up, due to densification of the core. Here, a sharp drop in force was observed in the unidirectional honeycomb samples, this being in contrast to the relatively steady decrease in force for the multidirectional samples.
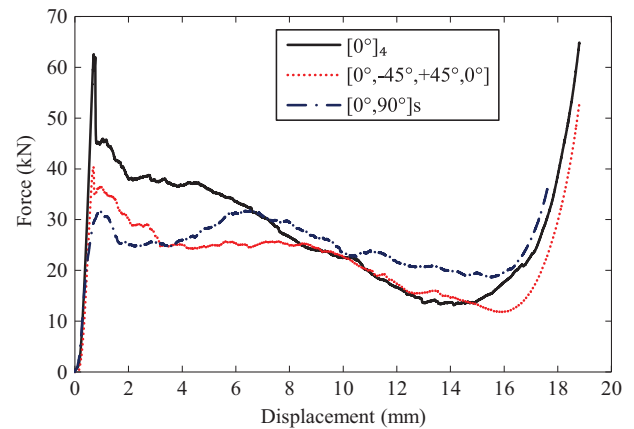

Figure 3. Typical force–displacement traces of one-cell honeycomb samples at crosshead displacement rate of 0.2 mm/min.

Table 1. Summary of the average values for one-cell honeycomb cores investigated in this study.

Sample codes	Orientations	Sample mass (g)	Loading rate (mm/min)	Strain rate (s^{-1})	Peak load (kN)	Compression strength (MPa)	Specific energy absorption (kJ/kg)
01-1	$[0°]_4$	7.6	0.2	0.00015	49.5	35.4	45.1
02-1	$[0°]_4$	7.9	20	0.015	53.6	38.3	53.7
03-1	$[0°]_4$	7.6	100	0.076	50.3	35.9	47.9
451-1	$[0°, -45°, +45°, 0°]$	8.0	0.2	0.00015	36.1	25.8	38.2
452-1	$[0°, -45°, +45°, 0°]$	7.9	20	0.015	33.8	24.2	37.9
453-1	$[0°, -45°, +45°, 0°]$	8	100	0.076	41.5	29.6	40.8
901-1	$[0°, 90°]s$	7.8	0.2	0.00015	33.5	23.9	45.2
902-1	$[0°, 90°]s$	8.0	20	0.015	37.3	26.6	52.8
903-1	$[0°, 90°]s$	8.0	100	0.076	43.1	30.8	53.4
21-1	$[0°]_4$	8.1	150,000	113.63	67.4	48.2	49.8
22-1	$[0°]_4$	8.0	240,000	181.82	63.6	45.5	52.8
23-1	$[0°]_4$	7.8	171,429	129.87	59.2	42.3	54.7
2451-1	$[0°, -45°, +45, 0°]$	7.8	240,000	181.82	59.1	42.2	45.6
2452-1	$[0°, -45°, +45°, 0°]$	7.8	171,429	129.87	52.3	37.3	40.1
2453-1	$[0°, -45°, +45 \text{ and } 0°]$	7.6	150,000	113.63	54.6	39.0	40.3
2901-1	$[0°, 90°]s$	8.1	240,000	181.82	52.3	37.3	43.2
2902-1	$[0°, 90°]s$	8.3	133,333	101.01	60.2	43.0	43.1
2903-1	$[0°, 90°]s$	8.0	171,429	129.87	50.0	35.7	44.0

Fibre weight fraction = 0.49, L × W × H (mm) = 40 × 35 × 22.

A comparison of the mechanical response of the single-cell samples with multiple cell samples was undertaken by conducting tests on five-cell honeycomb cores, and the results of these tests are given in Table 2. Figure 4 shows typical load–displacement graphs following tests on the five-cell honeycomb cores at a cross-head displacement rate of 0.2 mm/min. The graphs exhibit similar trends to those previously observed following tests on the one-cell honeycomb samples shown in Figure 3. Once again, the force increases linearly to a peak value whose magnitude reflects the increased number of cells in the samples. It is interesting to note that following the maximum in the graphs for the five-cell unidirectional honeycombs, the force drops more gradually than in the single-cell samples. The force during the middle stages of the test on the [0°, 90°]s sample remains relatively constant, similar to that observed following tests on aluminium-based honeycomb structures. Once again, continued loading results in crushing of the material and the load increases rapidly due to densification of the honeycomb structure.

A comparison of failure mechanisms between the one-cell and the five-cell unidirectional honeycomb samples at a compression rate of 0.2 mm/min is shown in Figure 5. Failure in the unidirectional sample involved the initiation of a number of vertical cracks, which are followed by delamination, resulting in the cell walls sliding outwards against the moving platen. The figure also shows failure in the form of fibre cracking in the one-cell sample and localized crushing at the lower surface in the five-cell sample causing the vertical cell wall to tilt sideways, precipitating vertical splits in the cell walls. The crushing processes can explain a sharp drop in force observed in the single unidirectional honeycomb samples, as shown in Figure 3, this being in contrast to the relatively steady decrease in force for the five-cell unidirectional honeycombs, as shown in Figure 4. Based on these observations between unidirectional honeycombs and the

Table 2. Summary of the average values for five-cell honeycomb cores investigated in this study.

Panel codes	Orientations	Sample mass (g)	Loading rate (mm/min)	Strain rate (s⁻¹)	Peak load (kN)	Compression strength (MPa)	Specific energy absorption (kJ/kg)
01-5	[0°]₄	24.3	0.2	0.00015	130.9	31.3	46.0
02-5	[0°]₄	24.4	2	0.0015	162.7	38.9	49.9
03-5	[0°]₄	23.7	20	0.015	156.3	37.4	64.4
04-5	[0°]₄	23.6	100	0.076	151.7	36.3	63.0
451-5	[0°, −45°, +45°, 0°]	23.6	0.2	0.00015	97.8	23.4	44.3
452-5	[0°, −45°, +45°, 0°]	24.0	2	0.0015	104.1	24.9	45.5
453-5	[0°, −45°, +45°, 0°]	23.6	20	0.015	116.3	27.8	54.9
454-5	[0°, −45°, +45°, 0°]	23.9	100	0.076	128.8	30.8	55.8
901-5	[0°, 90°]s	24.1	0.2	0.00015	96.5	23.1	46.2
902-5	[0°, 90°]s	23.8	2	0.0015	111.5	26.7	43.6
903-5	[0°, 90°]s	23.7	20	0.01515	110.4	26.4	50.6
904-5	[0°, 90°]s	24.0	100	0.076	131.2	31.4	57.6
21-5	[0°]₄	23.2	132,000	100.00	174.5	41.8	61.9
22-5	[0°]₄	23.5	131,000	99.24	176.9	42.3	55.2
23-5	[0°]₄	23.4	149,032	112.90	247.6	59.2	57.4
24-5	[0°]₄	22.5	190,667	144.44	256.8	61.4	57.9
2451-5	[0°, −45°, +45°, 0°]	23.0	112,500	85.23	155.6	37.2	44.9
2452-5	[0°, −45°, +45°, 0°]	23.6	121,481	92.03	170.9	40.9	43.0
2453-5	[0°, −45°, +45°, 0°]	22.5	127,500	96.59	179.6	43.0	52.1
2454-5	[0°, −45°, +45°, 0°]	22.3	190,385	144.23	237.8	56.9	49.9
2901-5	[0°, 90°]s	22.9	97,200	73.63	136.5	32.7	41.9
2902-5	[0°, 90°]s	22.6	101,481	76.88	148.2	35.4	46.7
2903-5	[0°, 90°]s	23.3	126,000	95.46	232.0	55.5	51.5
2904-5	[0°, 90°]s	23.3	191,949	145.42	252.8	60.5	51.9

Fibre weight fraction = 0.49, L × W × H (mm) = 74 × 56.5 × 22.

multidirectional samples, it is clear that off-axis fibres [0°, −45°, +45°, 0°] and [0°, 90°]s fibre stacking sequences serve to stabilise the deformation behaviour, thereby eliminating sudden catastrophic failure.
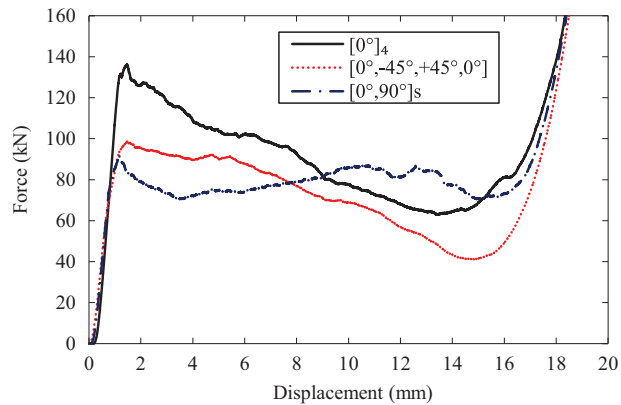

Figure 4. Typical force–displacement traces following compression tests on five-cell honeycomb cores at a crosshead displacement rate of 0.2 mm/min.

Figure 6 compares the compression strengths and SEA values for the one- and five-cell honeycomb cores based on the three stacking sequences at a displacement rate of 0.2 mm/min. The data for the single-cell samples show that the compression strength is highest in the samples based on the unidirectional core, reaching 35 MPa, while the tests on the [0°, −45°, +45°, 0°] and [0°, 90°]s yielded values that were 27 and 32 percent lower than that measured on the unidirectional system, respectively. Similar observations were made by Russell et al.[20] who reported that the compressive strength of a honeycomb structure depended on its fibre orientation. It is interesting to note that increasing the number of cells to five resulted in a drop in the compression strength for all stacking sequences. This may be due to the increased likelihood of the presence of strength-limiting defects in the larger samples. At quasi-static rates of loading, these structures offer values of SEA ranging from 38 to 46 kJ/kg, with the highest value being recorded for the five-cell [0°, 90°]s honeycomb. In contrast to the

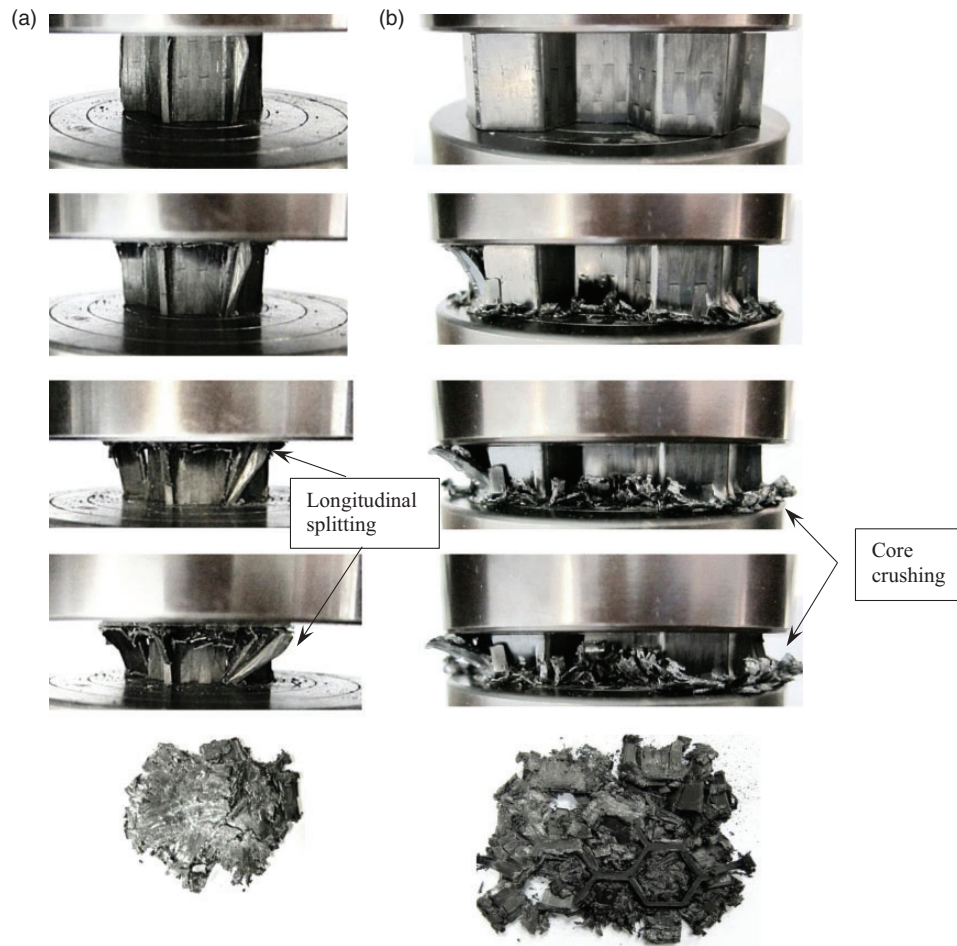**Figure 5.** Comparison of failure mechanisms in a one-cell and five-cell [0°]₄ sample during compression loading at a displacement rate of 0.2 mm/min.
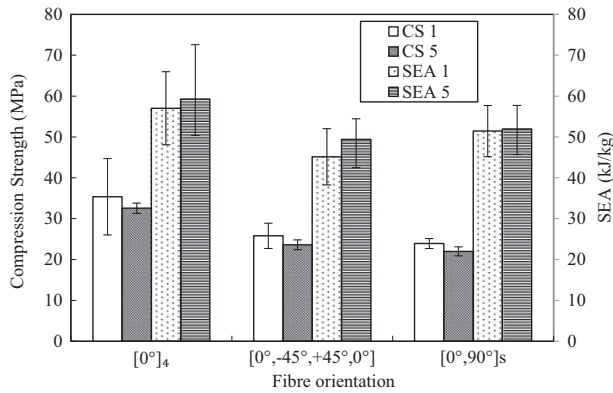
Figure 6. Bar chart plot showing the effect of stacking sequence on the compression strength and specific energy absorption of the one-cell and five-cell honeycomb cores at 0.2 mm/min.

SEA: specific energy absorption.

Figure 7. Typical force–displacement traces of the one-cell honeycomb samples at average impact loading rate of 162,857 mm/min.

Figure 8. Photographs of failure mechanisms in the one-cell samples subjected to various impact energies. (a) Impact energy 485 Joules on the one-cell honeycomb cores $[0°]_4$; (b) Impact energy 327 Joules on the one-cell honeycomb cores $[0°, -45°, +45°, 0°]$; (c) Impact energy 407 Joules on the one-cell honeycomb core $[0°, 90°]s$.

compression strength data, it is clear that in all cases, the SEA values of the five-cell cores are higher than their single-cell counterparts. This may be a result of the presence of the adjacent cells, which offer greater levels of support to the honeycombs by reducing the lateral movement of the cell walls, as previously observed in Figure 5.

Influence of loading rate on the energy-absorbing characteristics of the CFRP honeycombs

Single-cell samples. Here, attention centred on investigating the strain rate sensitivity of single-cell honeycomb samples through a series of dynamic tests at loading rates of up to 5 m/s. The impact energies were increased up to 485 J in order to fully crush the samples. The force–displacement graphs following impact loading on samples with fibre stacking sequences of $[0°]_4$, $[0°, -45°, +45°, 0°]$ and $[0°, 90°]s$ are shown in Figure 7, and the results of these tests are given in Table 1. All graphs exhibit similar features, with the force increasing to a peak value, followed by a significant drop and then a highly oscillatory response, due to ringing effects in the load cell and oscillations in the impact carriage. A comparison of the graphs for the three cores indicates that the unidirectional honeycomb offers peak force and the plateau values that are between 30 and 50% higher than its two counterparts. The dynamic responses of the three samples exhibit similar trends to the quasi-static graphs shown in Figure 3. In addition, the $[0°]_4$ samples offer superior compression strengths and energy-absorbing properties to the multidirectional samples.

An examination of the fractured honeycomb samples shown in Figure 8 indicates that the crushing process leads to splitting, delamination and fibre fracture,
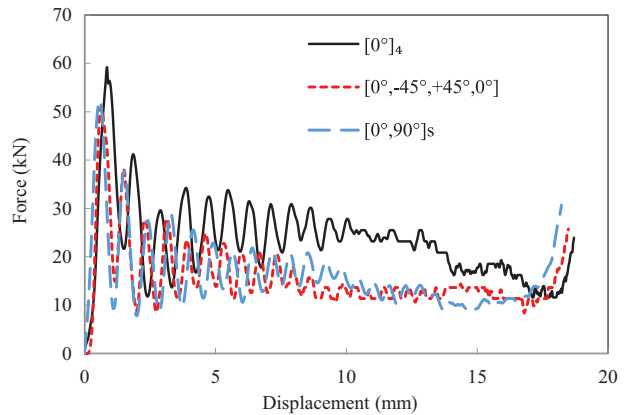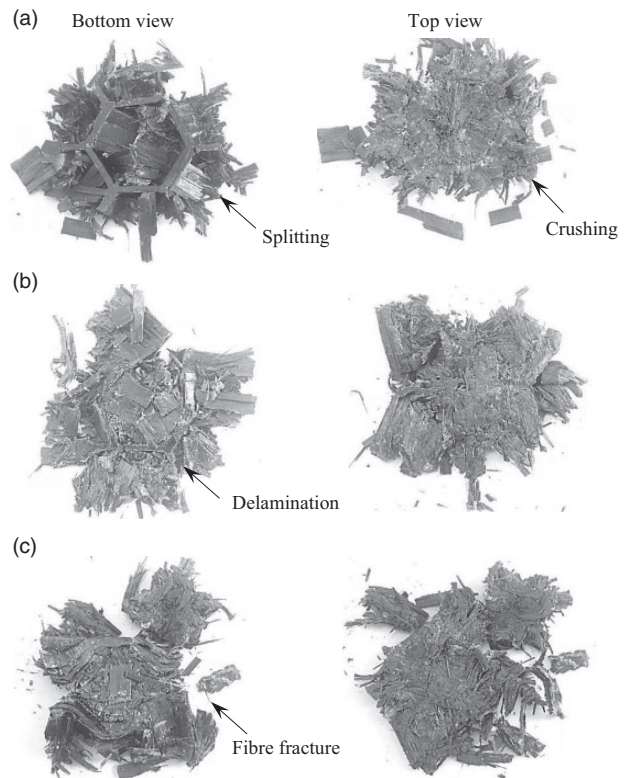
mechanisms that are similar failure modes to those observed elsewhere following tests on roll-wrapped carbon/glass fibre-reinforced composite cylinders.[25] It is clear that the $[0°]_4$ hexagonal sample exhibits greater numbers of larger rectangular-shaped platelets

(Figure 8(a)) than the [0°, −45°, +45°, 0°] and [0°, 90°]s samples (Figure 8(b) and (c)). The [0°]₄ sample was crushed to approximately 80% at an impact energy of 485 J, whereas the [0°, −45°, +45°, 0°] and [0°, 90°]s samples were crushed completely at impact energies of 327 and 407 J, respectively.

Figure 9 compares the dynamic and quasi-static load–displacement graphs for the [0°]₄ and [0°, −45°, +45°, 0°] one-cell cores. A similar overall response to that observed following quasi-static testing on these structures is apparent, where a rapid increase in load to a maximum value followed by a sudden drop and continued crushing until the structure densifies and the load increases sharply once more. An obvious feature in the load–displacement graphs in the dynamic tests is a series of oscillations, an effect that is attributed to ringing in the load cell. As expected, the [0°]₄ sample is stronger than the [0°, −45°, +45°, 0°] core, with the initial stiffness being similar under dynamic and quasi-static loading conditions.

A comparison of the maximum strengths of these two types of core shows that the strength of the [0°]₄ core is similar at both rates, whereas the [0°, −45°, +45°, 0°] core exhibits a higher strength under dynamic

conditions. Previous work using the Split Hopkinson bar technique has shown that unidirectional carbon fibre composites tend to be rate insensitive.[26] Orienting the fibres at off-axis angles, such as in the [0°, −45°, +45°, 0°] samples, introduces resin-dominated effects, including shear deformations in the epoxy matrix, that are likely to be highly sensitive to strain rate. These observations are likely to explain the differences in the rate-sensitive responses of the unidirectional and multidirectional composites.[27,28] For the [0°]₄ core, the dynamic curve appears to plateau at a roughly constant value, this being in contrast to the corresponding quasi-static curve that shows a steady decrease. It can be seen that the dynamic curve for the [0°, −45°, +45°, 0°] core is lower than the quasi-static trace, suggesting a lower energy absorption. For both cores, the densification threshold is delayed slightly at dynamic rates due to some failed fragments being ejected which contribute to a slightly higher crush displacement before densification.

The variation of the compression strength of one-cell samples, based on the three stacking sequences as a function of crosshead displacement rate, is shown in Figure 10. The impact velocities adopted in these tests
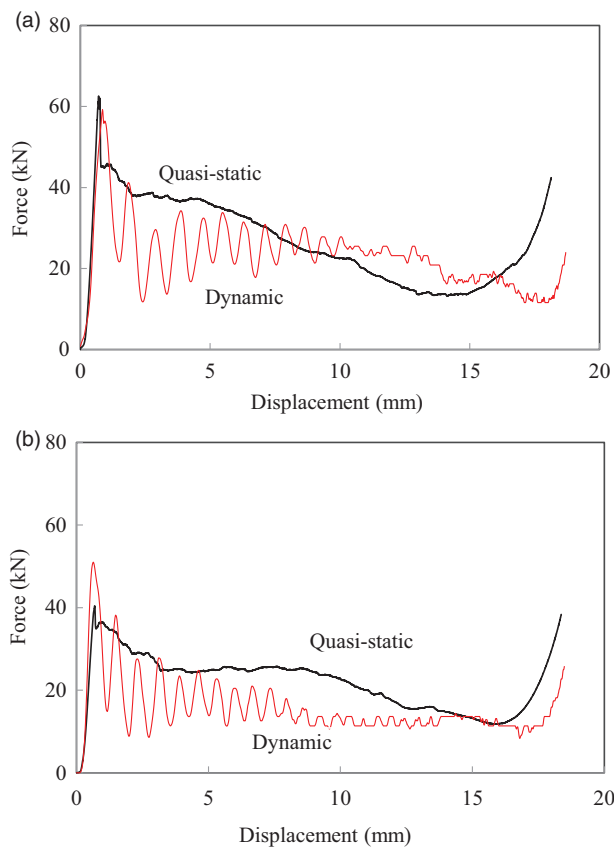

Figure 9. Comparison of the dynamic and quasi-static load–displacement traces for the one-cell cores.
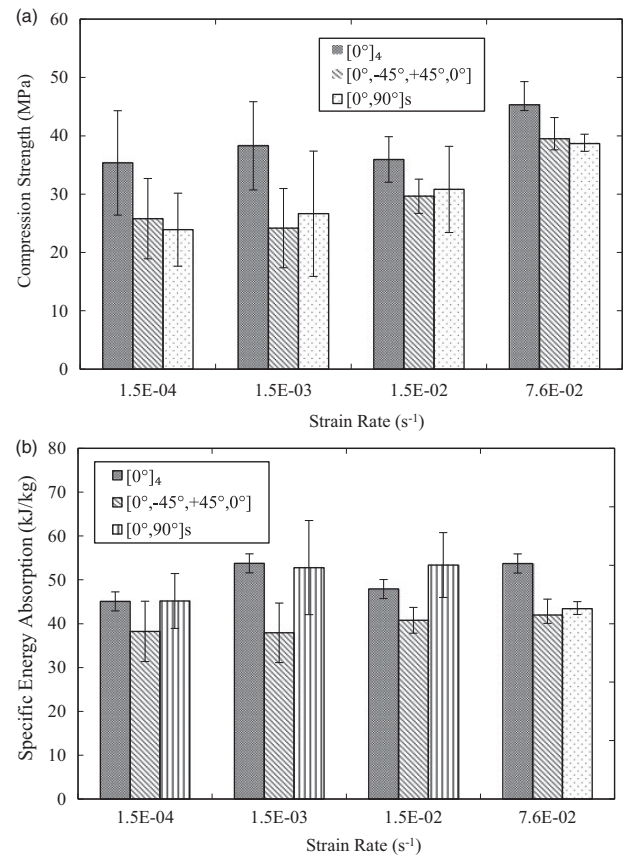

Figure 10. Variation of (a) the compression strength and (b) the SEA with strain rate for the one-cell honeycomb cores.

ranged from 4 to 5 m/s, resulting in a crushing time that varied from 5 to 8 ms. From the Figure 10(a), it is clear that the strength of the unidirectional samples is relatively stable, with values averaging approximately 45 MPa over the range of test conditions considered. In contrast, those samples based on off-axis fibres exhibit a rate-dependency with the strength tending to increase with strain rate. This is due to viscoelastic effects in the epoxy resin and the rate-sensitive nature of the fracture properties of the fibre–matrix interface. Both the [0°, −45°, +45°, 0°] and [0°, 90°]s cores exhibit similar strengths that are clearly lower than those measured on the unidirectional samples. Figure 10(b) shows the variation of SEA with crosshead displacement rate for the three stacking sequences. An examination of the figure indicates that the SEA values remain reasonably constant with increasing crosshead displacement rate. In most cases, the [0°]4 samples offer higher values of SEA with the highest value recorded being approximately 65 kJ/kg. This evidence suggests that the overall values of SEA for the dynamically loaded CFRP honeycomb are encouraging and higher than values measured on other cores, such as aluminium

honeycomb is 19 kJ/kg approximately,[29] and Nomex is 21 kJ/kg approximately[30] in earlier study.

Multicell samples. The dynamic behaviour of the five-cell honeycomb cores was then investigated through drop-weight impact tests at impact energies up to 1200 J, and the results are given in Table 2. Figure 11 compares the force–displacement graphs following compression tests at quasi-static and impact rates of loading (0.2, 2, 20, and 100 mm/min) on the unidirectional [0°]4 and the [0°, −45°, +45°, 0°] five-cell honeycomb core samples. The force–displacement graphs at rates below 100 mm/min are similar. Following the peak in the force, the load decreases as the honeycombs are continuously crushed until they reach the densification threshold. The graphs indicate that the initial stiffness and peak force values increase with loading rate, which again demonstrate the rate-dependent response of the cores. Figure 12 shows the failure modes in the [0°]4 and
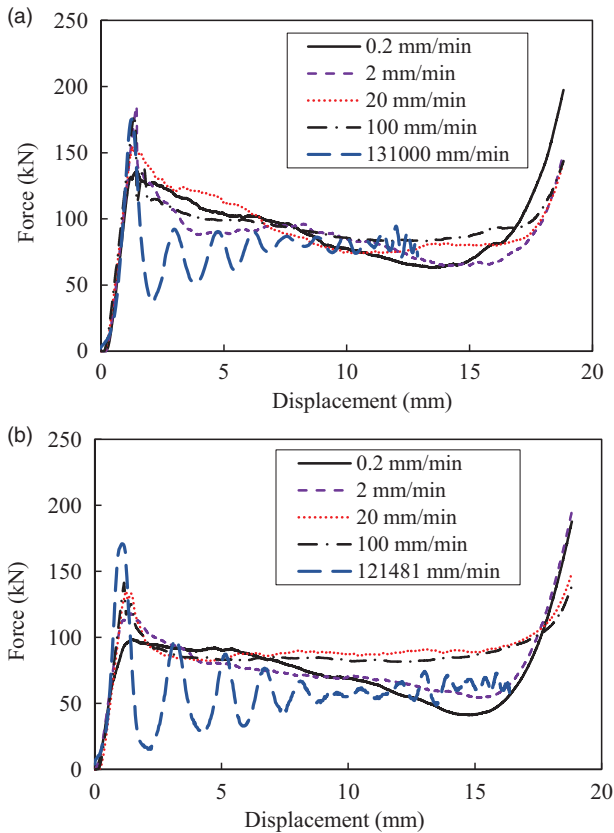

Figure 11. Force–displacement traces following compression tests on the five-cell honeycomb cores at increasing displacement rate (a) [0°]4 samples and (b) [0, ±45°, 0] samples.
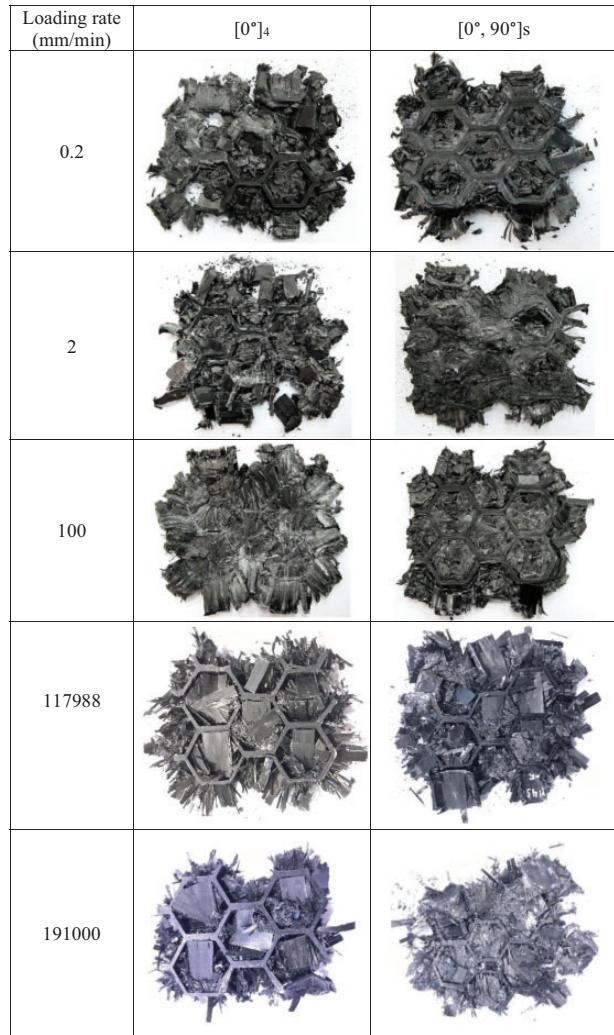

Figure 12. Photographs of the failed unidirectional and failed [0°, 90°]s samples at different rates.

$[0°, 90°]s$ samples at different loading rates. Whereas at quasi-static loading rates, the honeycomb cores were fully crushed, and however, at the impact loading rates this was not the case.

A comparison of the variation compression strength with loading rate for the three stacking sequences of the five-cell honeycomb cores is shown in Figure 13. As with the one-cell honeycomb, the evidence suggests that the strengths of the $[0°]_4$ core is relatively rate-insensitive. Again, there is a trend for the compression strength to increase with crosshead displacement rate for samples that are based on off-axis fibres. Figure 13(a) shows that the strength of the $[0°, -45°, +45°, 0°]$ approaches the $[0°]_4$ at impact rates of loading. This evidence suggests that rate effects in the resin and at the fibre–matrix interface are responsible for the increasing strength. Figure 13(b) shows the values of SEA for the three stacking sequences of the five-cell honeycomb structures with increasing loading rate, where it is clear that the unidirectional cores out-perform their multi-axis counterparts. Overall, the SEA values remain reasonably constant with increasing strain rate. It is worth noting that the values are higher than the single-cell samples, due to the higher level of constraint associated with the presence of

neighbouring cells in these five-cell structures. The resulting SEA values of 60 kJ/kg are encouraging for continuous core materials. The higher energy absorption in the $[0°]_4$ cores is due to a combination of splaying and interlaminar delamination mechanisms occurring within the honeycomb structures.

Conclusions

The compressive properties of composite honeycomb cores manufactured using the VARTM technique have been studied over a wide range of strain rates. Initial attention was paid on the compression strength and energy-absorbing response of one- and five-cell honeycomb samples subjected to quasi-static loading. The results indicate that one-cell samples, based on three stacking sequences, yielded a higher compression strength than five-cell cores, with the highest values being recorded following tests on samples based on the unidirectional $[0°]_4$ core. Here, higher SEA values were obtained in five-cell samples possibly as a result of the greater levels of support provided by the adjacent cells. Tests at impact rates of loading highlighted the fact that the strength of the $[0°]_4$ samples was relatively insensitive to strain rate, whereas a positive rate sensitivity was observed in the multidirectional samples. Failure processes occurring during compression were observed in the form of fibre fracture and localized crushing, tilting of the walls and vertical splits in the cell walls. In terms of SEA, the values were found to be reasonably constant over the range of strain rates considered here for all core structures. Tests on unidirectional and multi-axis composite honeycomb cores have shown that these structures offer attractive compressive and energy absorbing characteristics that are suited for applications where significant amount of energy need to be absorbed in a short-time scale.
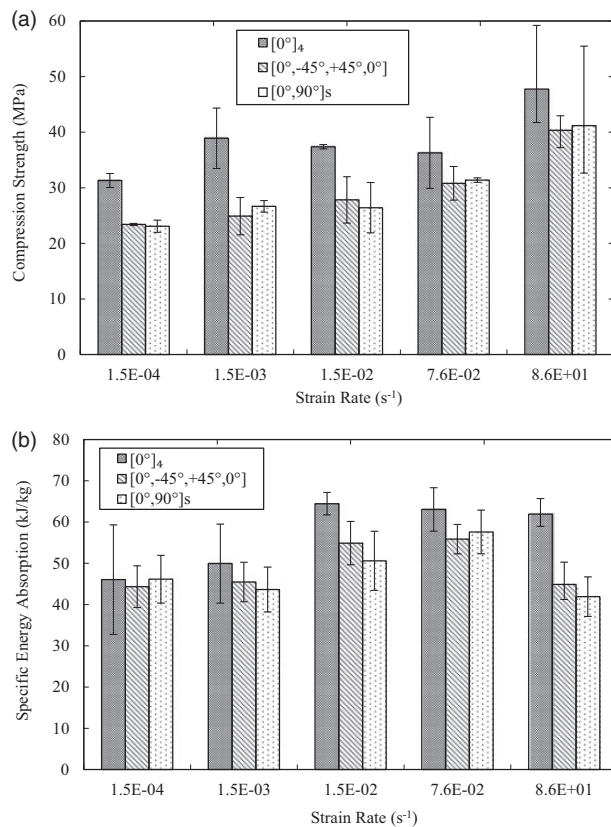

Figure 13. Variation of (a) the compression strength and (b) the SEA with strain rate for the five-cell honeycomb cores.

ORCID iDs

RA Alia https://orcid.org/0000-0002-4717-8258
J Zhou https://orcid.org/0000-0003-0584-3894

References

1. Goldsmith W and Sackman JL. An experimental study of energy absorption in impact on sandwich plates. *Int J Impact Eng* 1992; 12: 241–262.

2. Wu E and Jiang WS. Axial crush of metallic honeycombs. *Int J Impact Eng* 1997; 19: 439–456.

3. Foo CC, Chai GB and Seah LK. Quasi-static and low-velocity impact failure of aluminium honeycomb sandwich panels. *P I Mech Eng L-J Mat* 2006; 220: 53–66.

4. Hong ST, Pan J, Tyan T, et al. Dynamic crush behaviors of aluminum honeycomb specimens under compression dominant inclined loads. *Int J Plast* 2008; 24: 89–117.

5. Zhao H and Gary G. Crushing behaviour of aluminium honeycombs under impact loading. *Int J Impact Eng* 1998; 21: 827–836.

6. Meran AP, Toprak T and Mugan A. Numerical and experimental study of crashworthiness parameters of honeycomb structures. *Thin-Walled Struct* 2014; 78: 87–94.

7. Wang Z, Tian H, Lu Z, et al. High-speed axial impact of aluminum honeycomb – experiments and simulations. *Compos Part B: Eng* 2014; 56: 1–8.

8. Chen Y, Hou S, Fu K, et al. Low-velocity impact response of composite sandwich structures: modelling and experiment. *Compos Struct* 2017; 168: 322–334.

9. Aktay L, Johnson AF and Kröplin BH. Numerical modelling of honeycomb core crush behaviour. *Eng Fract Mech* 2008; 75: 2616–2630.

10. Xu S, Beynon JH, Ruan D, et al. Experimental study of the out-of-plane dynamic compression of hexagonal honeycombs. *Compos Struct* 2012; 94: 2326–2336.

11. Finnegan K, Kooistra G, Wadley HNG, et al. The compressive response of carbon fibre composite pyramidal truss sandwich cores. *Int J Mater Res* 2007; 98: 1264–1272.

12. Fan HL, Meng FH and Yang W. Sandwich panels with Kagome lattice cores reinforced by carbon fibres. *Compos Struct* 2007; 81: 533–539.

13. Fan H, Yang L, Sun F, et al. Compression and bending performances of carbon fibre reinforced lattice-core sandwich composites. *Compos Part A: Appl Sci Manuf* 2013; 52: 118–125.

14. Zheng Q, Fan H, Liu J, et al. Hierarchical lattice composites for electromagnetic and mechanical energy absorptions. *Compos Part B: Eng* 2013; 53: 152–158.

15. Zheng J, Zhao L and Fan H. Energy absorption mechanisms of hierarchical woven lattice composites. *Compos Part B: Eng* 2012; 43: 1516–1522.

16. Xiong J, Zhang M, Stocchi A, et al. Mechanical behaviors of carbon fibre composite sandwich columns with three dimensional honeycomb cores under in-plane compression. *Compos Part B: Eng* 2014; 60: 350–358.

17. Xiong J, Vaziri A, Ghosh R, et al. Compression behavior and energy absorption of carbon fibre reinforced composite sandwich panels made of three-dimensional honeycomb grid cores. *Extreme Mech Lett* 2016; 7: 114–120.

18. Petrone G, Rao S, De Rosa S, et al. Initial experimental investigations on natural fibre reinforced honeycomb core panels. *Compos Part B: Eng* 2013; 55: 400–406.

19. Petrone G, Rao S, De Rosa S, et al. Behaviour of fibre-reinforced honeycomb core under low velocity impact loading. *Compos Struct* 2013; 100: 356–362.

20. Russell B, Deshpande V and Wadley H. Quasistatic deformation and failure modes of composite square honeycombs. *J Mech Mater Struct* 2008; 3: 1315–1340.

21. Russell BP, Liu T, Fleck NA, et al. The soft impact of composite sandwich beams with a square-honeycomb core. *Int J Impact Eng* 2012; 48: 65–81.

22. Park S, Russell BP, Deshpande VS, et al. Dynamic compressive response of composite square honeycombs. *Compos Part A: Appl Sci Manuf* 2012; 43: 527–536.

23. Vitale JP, Francucci G, Xiong J, et al. Failure mode maps of natural and synthetic fibre reinforced composite sandwich panels. *Compos Part A: Appl Sci Manuf* 2017; 94: 217–225.

24. Alia RA, Al-Ali O, Kumar S, et al. The energy-absorbing characteristics of carbon fiber-reinforced epoxy honeycomb structures. *J Compos Mater* 2019; 53: 1145–1157.

25. Zhou J, Guan Z and Cantwell WJ. The energy-absorbing behaviour of composite tube-reinforced foams. *Compos Part B* 2018; 139: 227–237.

26. Koerber H and Camanho PP. High strain rate characterisation of unidirectional carbon-epoxy IM7-8552 in longitudinal compression. *Compos Part A: Appl Sci Manuf* 2011; 42: 462–470.

27. Oguni K and Ravichandran G. Dynamic compressive behavior of unidirectional E-glass/vinylester composites. *J Mater Sci* 2001; 36: 831–838.

28. Shams A, Panteghini A, Bardella L, et al. A micromechanical model to study failure of polymer-glass syntactic foams at high strain rates. *Comput Mater Sci* 2017; 135: 189–204.

29. Al Antali A, Umer R, Zhou J, et al. The energy-absorbing properties of composite tube-reinforced aluminum honeycomb. *Compos Struct* 2017; 176: 630–639.

30. Alia R, Rao S, Umer R, et al. The crushing characteristics of reinforced Nomex honeycomb. *J Reinf Plast Comp* 2018; 37: 1267–1276.